Published in final edited form as:
Atherosclerosis. 2008 November ; 201(1): 76–84. doi:10.1016/j.atherosclerosis.2008.01.017.

Selective Estrogen Receptor Modulation Influences Atherosclerotic Plaque Composition in a Rabbit Menopause Model

Brian G. Choi, MD, MBA[*,†], **Gemma Vilahur, DVM, PhD**[*], **M. Urooj Zafar, MD**[*,†], **Luis Cardoso, PhD**[‡], **Daniel Yadegar, MD**[*], **Borja Ibanez, MD**[*], **James Tunstead, PhD**[†], **Juan F. Viles-Gonzalez, MD**[*], **Mitchell B. Schaffler, PhD**[‡], **Valentin Fuster, MD, PhD**[†], and **Juan J. Badimon, PhD**[*,†]

[*]Cardiovascular Biology Research Laboratory, Mount Sinai School of Medicine, New York, NY

[†]Zena and Michael A. Wiener Cardiovascular Institute, Mount Sinai School of Medicine, New York, NY

[‡]Leni and Peter W. May Department of Orthopaedics, Mount Sinai School of Medicine, New York, NY

Abstract

Objective—Osteoporosis trials suggest raloxifene decreased cardiovascular events in women with preexisting atherosclerosis. We assessed the hypothesis that selective estrogen receptor modulation induces plaque stability in “menopausal” animals.

Methods and Results—Atherosclerosis was induced in 42 ovariectomized New Zealand White rabbits by cholesterol feeding and mechanical injury. Animals were imaged by magnetic resonance (MRI) for baseline atherosclerosis, and randomized to control (OVX, n=12), raloxifene 35–60 mg/kg/day by diet admixture (RLX, n=24), or immediate sacrifice (n=6) for immunohistopathologic correlation of MRI. Six months later, rabbits underwent repeat MRI then sacrifice for micro-computed tomography (μCT) and molecular analysis. Unlike OVX, RLX reduced atheroma volume. Analysis for lesion inflammation revealed reductions in COX-2, MMP-1, MCP-1 expression and macrophage infiltration in RLX vs. OVX with concomitant upregulation of estrogen receptor α. μCT showed similar total vascular calcification between groups, but calcifications in RLX were less nodular with better radial organization (mean calcific arc angle 63 ± 7° vs. 33 ± 6° in OVX), the predicted result of a 53% increase in BMP-2.

Conclusions—Raloxifene treatment results in reduced lesion volume, enhanced mechanical stability of vascular calcification, and less inflamed lesions characterized by less macrophage infiltration and reduced COX-2, MMP-1 and MCP-1 expression.

Keywords

Atherosclerosis; Inflammation; Osteoporosis; Selective Estrogen Receptor Modulator (SERM); Vascular Calcification

Correspondence: Juan J. Badimon, PhD., One Gustave L. Levy Place, Box 1030, New York, NY 10029, (212) 241-8484 Voice, (212) 426-6962 Fax, juan.badimon@mssm.edu.

The past twenty years have seen the cardiovascular mortality rate for women surpass that for men, and the gap has continued to widen; today, 1 in 2 postmenopausal women have cardiovascular disease.[1] Attempts at narrowing this disparity have thus far been unsuccessful. The 20th century paradigm of postmenopausal cardiovascular protection from hormone therapy (HT), encapsulated in the 1993 National Cholesterol Education Program Adult Treatment Panel II recommendation of HT as a therapeutic option for hypercholesterolemia that has adjunctive cardiovascular benefit,[2] has since been refuted by multiple clinical trials despite its confirmed lipid-modifying effects.[3, 4]

Recent efforts at female-specific pharmacologic therapies have focused on selective estrogen receptor modulators (SERMs). Most pertinently, post-hoc analysis from an osteoporosis treatment trial in post-menopausal women (the Multiple Outcomes of Raloxifene Evaluation, MORE) found that those women at high-risk for coronary artery disease (*i.e.*, a secondary prevention population most likely to have established atherosclerotic lesions) treated with the SERM raloxifene had 40 percent fewer cardiovascular events than those on placebo.[5] The Raloxifene Use for the Heart (RUTH) study, which was a double-blind, placebo-controlled, randomized clinical trial of this SERM's use in a patient population without pre-specified osteoporosis did not confirm this benefit.[6, 7]

The mechanism of raloxifene's potential effects upon atherosclerotic lesions is not completely understood. Pre-clinical animal models have shown that raloxifene, similar to HT, inhibits atherosclerosis,[8, 9] but its effect upon vascular calcification is unknown. HT results in less calcified plaques[10] without clear reduction in cardiovascular events,[11] yet statins, a therapy with clear reductions in cardiovascular events, increase calcification.[12, 13]

As a bone-active drug used for the treatment of osteoporosis in post-menopausal women, raloxifene has been speculated to affect vascular calcification morphology. An *in vitro* model demonstrated that raloxifene increases bone-morphogenetic protein-2 (BMP-2) promoter activity.[14] BMP-2 is a potent bone morphogen, and *in vitro* studies suggest that vascular calcifications form in stripe-like ridges with BMP-2 upregulation whereas its downregulation would result in more nodular mineralization.[15] Statins, which have been demonstrated to reduce cardiovascular morbidity and mortality, also increase BMP-2.[16] It has been postulated that such morphological changes in vascular calcification affects plaque stability.[17]

The ideal SERM then for the prevention of cardiovascular events should reduce lesion size without increasing plaque instability. This study assessed the hypothesis that raloxifene limits characteristics of plaque vulnerability by reducing atherosclerotic burden, and decreasing plaque inflammation while enhancing the structure of vascular calcification in the osteoporotic animal.

METHODS

Experimental model of atherosclerosis

As raloxifene is used primarily in osteoporotic post-menopausal women, 42 female New Zealand White rabbits (Covance Research Products; Denver, Pennsylvania) were ovariectomized after sexual maturity (age 5 months, 3.3 ± 0.2 kg). One month post-operatively, aortic atherosclerotic lesions were induced by 9 months of 0.2% cholesterol-enriched rabbit diet (WIL Research Laboratories; Ashland, Ohio) and double balloon-induced aortic endothelial denudation as previously described.[18–23] All procedures were performed under general anesthesia by intramuscular injection of acepromazine (1 mg/kg;

Boehringer Ingelheim Vetmedica; St. Joseph, Missouri), ketamine (20 mg/kg; Fort Dodge Animal Health; Fort Dodge, Iowa), and xylazine (2 mg/kg; Lloyd Laboratories; Shenandoah, Iowa). This experimental model of atherosclerosis has reliably demonstrated reproducible development of advanced atherosclerotic lesions,[18–23] and the study protocol was approved by the Institutional Animal Care and Use Committee of the Mount Sinai School of Medicine.

Study design

After 9 months of atherosclerosis induction, the animals were randomized into four groups: (A) raloxifene (Eli Lilly & Company; Indianapolis, Indiana) 35 mg/kg/day admixed in 0.1% cholesterol diet for six months (Low RLX; n=12), (B) raloxifene 60 mg/kg/day admixed in 0.1% cholesterol diet for six months (High RLX; n=12), (C) a placebo-control group receiving 0.1% cholesterol diet alone (OVX; n=12) for six months, or (D) to immediate sacrifice for baseline atherosclerosis control (n=6). Previous pharmacokinetic data in rabbits have shown that the doses chosen have been demonstrated to produce plasma raloxifene concentrations in a similar range to those found in postmenopausal women treated with raloxifene.[9] Given the current mandate for statins as a mainstay of lipid-lowering therapy for atherosclerotic diseases, the cholesterol content of the diets was reduced during the treatment period (*i.e.*, after randomization) to mimic the hypolipidemic effect of statin therapy without potentially confounding pleiotropic effects associated with this drug class. Six months after randomization into the treatment groups, all rabbits were sacrificed for histopathology, molecular study and *ex vivo* micro-computed tomography (μCT). Development of osteoporosis was confirmed by μCT.[24, 25] All rabbits were imaged *in vivo* by magnetic resonance imaging (MRI) immediately prior to randomization and prior to sacrifice. The sample size was calculated to detect change in aortic vessel wall area as assessed by serial MRI (the pre-specified primary endpoint) based upon a power of 0.8 and α of 0.05, observations from a prior experimental model of raloxifene administration, and measurement error from prior MRI studies in our laboratory using the same experimental model.[9, 18–23] Observers for all measurements (MRI, histopathology, Western blot, platelet aggregometry and μCT) were blinded to treatment group.

In vivo magnetic resonance imaging of atherosclerotic lesions

The animals were anesthetized as above and placed supine in a 1.5-Tesla MRI system (Siemens Medical Solutions; Malvern, Pennsylvania) using a conventional extremity coil. Gradient-echo coronal and sagittal images were used to localize the abdominal aorta, and sequential transverse images (3-mm thickness) of the aorta were obtained from the celiac trunk to the iliac bifurcation using a fast spin-echo sequence (total imaging time 1 hour) with an in-plane resolution of 230 × 230 μm [proton density weighted (PDW): TR/TE, 2300/5.6 ms; T1W: TR/TE, 800/5.6 ms; T2W: TR/TE, 2300/62 ms; field of view 12 × 12 cm; matrix 512 × 512; echo train length = 8; signal averages = 4]. T1W sequence was repeated 5 minutes after injection of gadopentetate dimeglumine (0.1 mmol/kg; Berlex Laboratories; Montville, New Jersey). Fat suppression and flow saturation pulses were used as previously reported.[19]

The acquired MRIs were transferred to a Macintosh computer system (Apple; Cupertino, California) for analysis. The pre- and post-treatment images were matched for anatomic position by using distances from the renal arteries and iliac bifurcation as previously validated,[19] so that each animal served as its own control and true serial data on atherosclerotic progression/regression could be obtained. The 6 cm of aorta immediately distal to the left renal artery, corresponding to 20 contiguous MRI segments, were selected for vessel wall measurements. Cross-sectional areas of the lumen and vessel wall were determined by a validated semi-automatic quantification method programmed on ImageJ

(National Institutes of Health; Bethesda, Maryland) that determined the lumen area and vessel wall area (vessel wall area = total vessel area − lumen area); the intra-observer variability for vessel wall measurement using this automated program was 2.1%, indicating high reproducibility of measurement.[26] For each animal at each time point, measurements from the 20 contiguous MRIs were averaged, and the mean values for each rabbit were considered for statistical analysis.

Whole-blood platelet aggregation

Prior to euthanasia, whole blood was collected in 3.2% sodium citrate vacutainers by phlebotomy via the middle ear artery. Within an hour of phlebotomy, platelet aggregation to adenosine diphosphate (ADP; 10 and 20 μM) was performed in diluted whole blood by the impedance method using the Chrono-log 570VS aggregometer (Chrono-log; Havertown, Pennsylvania) as previously described.[27]

Micro-computed tomography of vascular calcification

Within 24 hours of the final MRI, the rabbits were euthanized by intravenous injection of 150 mg/kg sodium pentobarbital (Sleepaway; Fort Dodge Animal Health). Prior to euthanasia, the animals received heparin (100 U/kg; American Pharmaceutical Partners; Schaumberg, Illinois) to prevent post-mortem thrombosis. The aortas were cannulated at the level of the diaphragm and immediately flushed proximally and distally with 250 ml of 0.1M phosphate-buffered saline (PBS), pH 7.4. The abdominal aorta was further flushed with 250 ml of cold (4 °C) perfusion fixative at 100 mmHg (4% paraformaldehyde in PBS). Using anatomic landmarks observed by MRI, the abdominal aorta was excised, immersed in fresh fixative with preserved *in situ* configuration, and then stored at 4 °C for 1 week to fix the tissue. A 6-cm section distal to the left renal artery, which corresponded to the segment analyzed by MRI, was then washed free of formaldehyde using distilled water and immersed in PBS prior to μCT image acquisition. The potential of MRI to assess calcified tissue in blood vessels is limited by the nature of its principle of measurement. The presence of plaque calcifications is determined by the absence of signal intensity on MRI sequences as a consequence of the reduced number of water molecules in the mineralized tissue which are responsible for the resonance signal. However, not only calcified tissue results in lack of signal in MRI (*i.e.*, a black image), but also other components of an atherosclerotic lesion may exhibit weak signal intensity.[28, 29] Conversely, magnetic field inhomogeneities resulting from diamagnetic susceptibility between calcified and soft tissue have the potential to lead to overestimation of mineral presence on MRI.[30] In contrary, quantitative μCT is considered the gold standard for assessment of calcified tissue. The CT principle of measurement is based on the specific absorption to X-rays demonstrated by materials with different density (*e.g.*, air, water, lipid, mineral, etc.). When calibrated with adequate phantoms within the scan, images from μCT can provide true information about mineral density and mineral content in addition to mineral volume. For the above-mentioned reasons, the specificity of μCT to distinguish mineralized tissue is higher than the one exhibited by MRI. X-ray images of the aorta were obtained using a GE Healthcare eXplore SP Pre-Clinical Specimen Micro-CT system (General Electric; London, Ontario). For image acquisition, 360 consecutive X-ray projections were obtained using an exposure time of 1.7 seconds, at 80kVp and 80mA, and a voxel resolution of 21 μm. For each projection, five exposures were obtained and averaged to produce a high-contrast low-noise image. The raw images were corrected for possible pixel defects in the digital detector using bright and dark fields, and a standard reconstruction algorithm included in the GE analysis system was applied to generate three-dimensional volumes from the planar projections. Mineral density within the volumes was calibrated using a phantom containing hydroxyapatite, air and water, which was included with each scan. For the analysis of calcified tissue, the volume enclosing the entire 6-cm aorta segment was selected. Images were segmented into calcified

and non-calcified tissue on each volume of interest using a global threshold method.[31] After calibration and identification of calcified tissue, the amount of calcium in the sample was quantified using the Tissue Mineral Content tool in the Advanced Bone Analysis software from GE Healthcare. Mineral organization in the volume was assessed using a method based upon a previously established analysis by intravascular ultrasound (IVUS).[32] Three-dimensional images were reconstructed for the 20 contiguous 3-mm sections corresponding to the MRI slices; the largest arc of calcium in each cross-section was identified, and the arc was measured in degrees with a protractor centered on the vessel lumen (representative measurements seen in Figures 1C and 1F).

Histopathology and immunohistochemistry

Following μCT, the aortic segments analyzed by MRI and μCT were cut into 3-mm sections corresponding to the imaging analysis segments. Specimens were paraffin-embedded and cut into serial 5-μm thick sections. Within each 3-mm segment, a section was stained with Masson's trichrome elastic stain and additional sections stained immunohistochemically with estrogen receptor α (ERα) antibody (Lab Vision; Fremont, California); RAM-11 antibody for macrophages (Dako; Carpenter, California), α-actin for vascular smooth muscle cells (Sigma-Aldrich; Saint Louis, Missouri), and matrix metalloproteinase-1 (MMP-1; Lab Vision). The abdominal aorta superior to the left renal artery was separately processed by Oil Red O method for lipid deposition. Histopathologic analysis was performed using a computer-based quantitative color image analysis system (ImageJ) to assess the percentage of stained area for each section.

Western blot analysis

Immediately after euthanasia, the descending thoracic aorta was flushed with physiologic buffer as above and snap-frozen in liquid nitrogen. The frozen aortas were pulverized and homogenized in lysis buffer (50 mmol/L Tris-HCl, 1 mmol/L EDTA, 1% Triton X-100, 0.1 mg/ml PMSF, pH 7.4). Equal amounts of protein (50 μg/lane) estimated by bicinchoninic acid reagent (Pierce Biotechnology; Rockford, Illinois) were loaded in 10% PAGE to quantify protein expression. Western blot analysis was performed with antibodies against BMP-2 (Santa Cruz Biotechnology; Santa Cruz, California), cyclooxygenase-1 (COX-1; Transduction Laboratories; United Kingdom), cyclooxygenase-2 (COX-2; Transduction Laboratories), ERα (LabVision; Fremont, California), estrogen receptor β (ERβ; Santa Cruz Biotechnology), and monocyte chemoattractant protein-1 (MCP-1; Santa Cruz Biotechnology). After incubation with their respective peroxidase-labeled immunoglobulins, antibody visualization was performed by the chemiluminescent method SuperSignal® (Pierce Biotechnology) and evaluated by densitometry (ImageJ).

Statistical analysis

Measurements with multiple observations per rabbit (*i.e.*, MRI, μCT, histopathology) were averaged so that each rabbit represented a single observation per timepoint. Paired *t*-test was used for the serial MRI measurements to compare within groups the change from randomization to study conclusion. After testing for normal distribution and equality of variances with Levene's *F* test, unpaired *t*-test was used for all single timepoint measurements (*i.e.*, μCT, histopathology, Western, aggregometry) to compare between OVX and RLX. Secondary sub-group analyses by treatment dose (*i.e.*, OVX vs. Low RLX vs. High RLX) were performed using an overall model error and a Bonferroni adjustment for multiple comparisons (SPSS v11.0.2; Chicago, Illinois). All probabilities are two-sided with $p<0.05$ considered statistically significant. All values are expressed as mean ± standard error of the mean (SEM) or percent change from randomization.

RESULTS

Effects on plasma lipid levels and body weight

Dyslipidemia was improved in the raloxifene-treated animals without statistically significant differences between low RLX and high RLX (Table 1). After six months of treatment, although no significant difference was noted in total cholesterol, LDL-cholesterol, or high-density lipoprotein cholesterol (HDL), RLX had a more favorable 29% lower LDL:HDL ratio. There were no significant differences in body weight at baseline or end-of-follow-up, and effects on uterine weight similar to those previously established with raloxifene were observed.[9]

Changes in vessel wall measured by serial MRI

Significant regression in vessel wall area of −5.5 ± 4.5% between baseline and end-of-follow-up was seen in RLX, but no significant change was seen in OVX (Table 2). Comparison of pre-treatment versus post-treatment images revealed no significant change in lumen area in any of the groups (Table 2).

Qualitative analysis of plaque composition by multi-contrast MRI suggested increased lipid deposition (higher signal intensity in T1W and PDW and lower in T2W) in OVX compared to RLX. Vascular calcification (low signal intensity in T1W, T2W and PDW) in the RLX-treated groups was organized in a more circular, concentric manner than in OVX, which showed more nodular calcifications (Figure 1). The confluence of the mineralization gave the RLX-treated aortas the appearance of “auto-stenting” by calcification, resembling a tubular circumferential ring within the neointima (Figures 1B, 1C). To confirm these differences in calcification, all aortas were examined by μCT.

Vascular calcification assessment by μCT

The decrease in mineralization, both by weight and particle number, seen in RLX was not statistically significant (Table 3). In all groups, the areas of calcification predominated in the neointima (Figure 3). With the better image resolution of μCT and superior specificity of this methodology for calcification matched to a hydroxyapatite phantom, we confirmed the observations from MRI that the calcifications in the raloxifene groups had significantly greater arcs of calcium deposition than OVX (Table 3). The mean arc angle in OVX was approximately half that of the RLX groups. The calcifications in OVX were more nodular in appearance (Figures 1C, 1F).

Plaque composition by histopathology

Confirming the observation by MRI, post-mortem histopathologic analysis demonstrated a 35% reduction in lipid content (Oil Red O) and a 37% reduction in macrophage area (RAM-11) with raloxifene therapy as seen in Figure 2. No statistically different observations were made for smooth muscle content (α-actin). Representative immunohistopathology photomicrographs with corresponding μCT are presented in Figure 3.

Plaque protein expression

Raloxifene treatment resulted in increased expression of BMP-2 (Table 3) by 53% compared to OVX, which may explain the mineralization patterns seen by MRI and μCT. MMP-1 positive area (representative photomicrograph in Figure 3 and data presented in Figure 4) decreased in a dose-dependent manner with raloxifene treatment (OVX 38.3 ± 7.6%, Low RLX 24.9 ± 3.4%, High RLX 14.5 ± 2.9%). This pattern mirrored that of MCP-1 protein expression (Figure 4). Raloxifene treatment was also associated with reduced MCP-1 expression by 27% compared to OVX with more significant reduction in the High RLX

group, $p<0.001$. Furthermore, raloxifene appeared to reduce COX-2 expression (Figure 4) by approximately 60% compared to OVX. As expected, no differences were seen in the constitutive COX-1 (Figure 4). The effects on BMP-2, COX-2, MCP-1, and MMP-1 dovetailed with the approximately doubled ERα expression seen in the raloxifene-treated groups (Figure 4). Raloxifene at the concentrations in this study is more specific to ERα than ERβ,[33] but the marginal increase in ERβ seen in the High RLX group was not statistically significant (Figure 4). As seen in Figure 5, the increased ERα expression was specific to the inflammatory infiltrative cells.

Whole-blood platelet aggregation

ADP-induced platelet aggregation in the raloxifene-treated groups was significantly lower. When stimulated by ADP 10 μM, RLX aggregation was 1.3 ± 0.4Ω versus 3.6 ± 0.4Ω for OVX; when stimulated by ADP 20 μM, RLX aggregation was 1.6 ± 0.4Ω versus 4.8 ± 0.4Ω for OVX.

DISCUSSION

Our study may indicate that raloxifene not only induces *in vivo* regression of established atherosclerotic lesions but also alters plaque morphology and activity to a more stable phenotype in the setting of concomitant osteoporosis. If raloxifene treatment in humans results in the same conformational and metabolic changes in the vessel wall as seen in our model, we would expect to see a reduction in the likelihood of plaque rupture and subsequent acute coronary syndrome (ACS).

This study is also the first to provide *in vivo* evidence of BMP-2 upregulation resulting in linear vascular mineralization as was predicted by mathematical models in an *in vitro* study[15] and the first to demonstrate that vascular calcification is pharmacologically modifiable *in vivo*. The greater specificity and order-of-magnitude image-resolution advantage of μCT over MRI allowed superior *in situ* characterization of calcification morphology. The mineralization in the raloxifene-treated aorta conforms to a more “stent-like” intimal mechanical scaffold – concentric and continuous versus nodular and discontinuous as in the control animals. Regarding plaque composition, we confirmed prior experimental observations of decreased lipid deposition in raloxifene-treated rabbits[9] and also observed decreased macrophage infiltration in the vascular wall as predicted by *in vitro* study of human coronary artery endothelial cells treated with raloxifene.[34] Even though BMP-2 upregulation has been associated with decreased vascular smooth muscle cell growth,[16] we only observed a non-significant trend in this direction. Plaque activity was consistent with a reduction in inflammation in RLX as seen by significant reductions in MMP-1, MCP-1 and COX-2 (an inflammatory-induced COX isoform) [35]. A concern for COX-2 inhibition is a potential pro-thrombotic effect resulting in increased cardiovascular events.[36] Despite its COX-2 inhibitory effect, raloxifene did not result in greater arterial platelet aggregation, implying either that the scope of the COX-2 inhibition is confined within the lesion and does not significantly affect prostacyclin release or result in unopposed thomboxane-A2 upregulation or that raloxifene otherwise independently exerts some anti-platelet effect, as suggested by other experimental models.[37, 38] This result suggests that although raloxifene is known to be pro-coagulatory and increase venous thomboembolic events,[39] in the higher shear arterial system in which platelets play a greater role in thrombotic complications, raloxifene treatment reduces a platelet-derived prothrombotic potential.

Given the mild hypolipidemic effect of raloxifene therapy,[40] the modest reduction in vessel wall area compared to more robust lipid-lowering therapies such as statins was not unexpected.[41] Multiple animal studies have demonstrated that raloxifene reduces the size of

atherosclerotic lesions,[8, 9] and pursuant to these other studies, perhaps the marginal changes in lipid parameters (LDL reduction, HDL elevation) may have contributed to the differences in lipid deposition seen in this experiment. Alternatively, the atheroma regression may have occurred completely independent of systemic cholesterol levels and may have been mediated via the anti-inflammatory effects seen in vascular wall.[18]

Our study reveals an anti-inflammatory effect of raloxifene in the atherosclerotic lesion, possibly mediated by ERα as suggested by its increased protein expression, specific localization to inflammatory cells within the atherosclerotic vessel, and ERα's known role in atheroprotective effects.[42] Down-regulation of COX-2 in the vessel wall would decrease prostaglandin E_2 release, which may explain the relative MMP inactivity seen in the raloxifene-treated animals. With less MMP, the vessel is subject to less enzymatic activity, matrix degradation and mononuclear cell infiltration, corroborated by the decrease seen in MCP-1 in the raloxifene groups; the ultimate result confirmed by decreased macrophage content seen in the vessel wall. Therefore, the plaques in the raloxifene-treated animals have less macrophage infiltration than in the controls who have unopposed inflammation.

Furthermore, the more evenly distributed calcifications with greater confluence and radial organization than the nodular pattern seen in the controls may be explained by the fact that raloxifene is a known upregulator of BMP-2.[14] Upregulation of this morphogen predisposes vascular mesenchymal cells to self-organize into regularly spaced, stripe-like ridges whereas BMP-2 downregulation results in spot calcification.[15] This radial organization of the calcification may render the plaque more stable. Fujii *et al* demonstrated in an *in vivo* IVUS study of human coronary arteries that longer arcs of calcification are less likely to be found in ruptured lesions.[32] In terms of physics, the moment of inertia is increased rendering the vessel less likely to torque and generate higher shear stresses. Also, discontinuous, nodular calcifications result in greater von Mises stress creating more mechanical instability at the calcifications' interface with its neighboring softer non-calcified tissue.[17] Plaques with confluent concentric calcifications are less likely to rupture than those with discontinuous nodular ones, and while raloxifene did not result in a significant reduction of mineral quantity, the mineral organization was more stable.

Limitations

This translational animal study allowed us to investigate the effect of raloxifene on vessel anatomy by serial imaging as well as to gain insight into the mechanism behind this SERM's effects. An obvious limitation of this study is that prior pre-clinical studies with HT failed to predict accurately the outcomes of the major randomized clinical trials, although the reason for failure may be that the randomized controlled trials were not designed to repeat the conditions of the preclinical studies. RUTH, unlike MORE, did not prespecify for osteoporosis, and our model more closely mimicked the MORE population with concomitant atherosclerosis and osteoporosis. Nevertheless, the dual anti-atherogenic and anti-inflammatory effects, as well as the less mechanically disruptive calcification, seen with this SERM suggest that raloxifene may not increase plaque rupture.

Thought was given to the possibility that the more confluent calcification may result in "stove pipe" vessels unable to adapt to pulsatile flow, but the amount of calcification appears to be less in the raloxifene-treated groups in a dose-dependent manner compared to the ovariectomized controls. A limitation of this study is that the dose-dependent trend in vascular calcification is not statistically significant; the study may not have been sufficiently powered to detect this effect as this was not a pre-specified endpoint. Given the anti-inflammatory effect, one would have expected to see less calcification with raloxifene therapy since soft tissue calcification generally occurs in areas of chronic inflammation.[17] Even if the amount of calcification was equal between the groups, though, vulnerability to

rupture from “stent-like” calcific scaffolding is likely lower than that from the nodular variety.

An additional limitation of this study is the reliance of ovariectomy as a surrogate for menopause. The postmenopausal ovary is not endocrinologically inert,[43] but animal models of menopause rely upon surgical ovariectomy as a matter of necessity and expediency since mammalian survival after age-dependent ovarian failure is brief with the notable exception of humans, whose post-menopausal survival may be as much as one-third of lifespan.[44, 45] These factors make study of “natural” menopause in the aged mammal logistically difficult. Nevertheless, our results provide insight into the mechanism of raloxifene in the absence of gonadally produced endogenous sex hormones.

Conclusion

Our data show that treatment of established atherosclerotic lesions with raloxifene in this experimental *in vivo* model results in plaque regression and reduction of lesion vulnerability via anti-inflammatory effects and enhanced vascular calcification morphology. A confirmatory clinical trial of raloxifene in osteoporotic women with established atherosclerotic disease may establish whether these changes translate into true clinical benefit.

Acknowledgments

This study was made possible by NIH grants SCOR HL54469 and R01 HL071264 (to Drs. Fuster and Badimon), NHLBI grant T32 HL007824 (to Dr. Choi), a Spanish Ministry of Science & Education grant (to Dr. Vilahur), and an investigator-initiated research grant from Lilly Research Laboratories. The authors thank Jose Rodriguez, MD, and Constantin Novoselsky, MD, for their help in the surgical procedures; Anthony Lopez for expert planimetry; Barbara Bonacasa, PhD, and Boris Cortes, MD, for assistance with the molecular studies; and David Cox, PhD, and Mary Jane Geiger, MD, PhD, Eli Lilly & Company, for unrestricted support throughout this project. The authors would like to give special thanks to Gregg Goldschlager, DVM, Reginald Miller, DVM, and the staff of the Mount Sinai Center for Comparative Medicine & Surgery for dedicated animal care.

References

1. Thom T, Haase N, Rosamond W, Howard VJ, Rumsfeld J, Manolio T, Zheng ZJ, Flegal K, O’Donnell C, Kittner S, Lloyd-Jones D, Goff DC Jr, Hong Y, Adams R, Friday G, Furie K, Gorelick P, Kissela B, Marler J, Meigs J, Roger V, Sidney S, Sorlie P, Steinberger J, Wasserthiel-Smoller S, Wilson M, Wolf P. Heart Disease and Stroke Statistics--2006 Update. A Report From the American Heart Association Statistics Committee and Stroke Statistics Subcommittee. Circulation. 2006
2. Summary of the second report of the National Cholesterol Education Program (NCEP) Expert Panel on Detection Evaluation Treatment of High Blood Cholesterol in Adults (Adult Treatment Panel II). Jama. 1993; 269:3015–3023. [PubMed: 8501844]
3. Grady D, Herrington D, Bittner V, Blumenthal R, Davidson M, Hlatky M, Hsia J, Hulley S, Herd A, Khan S, Newby LK, Waters D, Vittinghoff E, Wenger N. Cardiovascular disease outcomes during 6. 8 years of hormone therapy: Heart and Estrogen/progestin Replacement Study follow-up (HERS II). Jama. 2002; 288:49–57. [PubMed: 12090862]
4. Rossouw JE, Anderson GL, Prentice RL, LaCroix AZ, Kooperberg C, Stefanick ML, Jackson RD, Beresford SA, Howard BV, Johnson KC, Kotchen JM, Ockene J. Risks and benefits of estrogen plus progestin in healthy postmenopausal women: principal results From the Women’s Health Initiative randomized controlled trial. Jama. 2002; 288:321–333. [PubMed: 12117397]
5. Barrett-Connor E, Grady D, Sashegyi A, Anderson PW, Cox DA, Hoszowski K, Rautaharju P, Harper KD. Raloxifene and cardiovascular events in osteoporotic postmenopausal women: four-year results from the MORE (Multiple Outcomes of Raloxifene Evaluation) randomized trial. Jama. 2002; 287:847–857. [PubMed: 11851576]

6. Mosca L, Barrett-Connor E, Wenger NK, Collins P, Grady D, Kornitzer M, Moscarelli E, Paul S, Wright TJ, Helterbrand JD, Anderson PW. Design and methods of the Raloxifene Use for The Heart (RUTH) study. Am J Cardiol. 2001; 88:392–395. [PubMed: 11545760]
7. Barrett-Connor E, Mosca L, Collins P, Geiger MJ, Grady D, Kornitzer M, McNabb MA, Wenger NK. Effects of raloxifene on cardiovascular events and breast cancer in postmenopausal women. The New England journal of medicine. 2006; 355:125–137. [PubMed: 16837676]
8. Bjarnason NH, Haarbo J, Byrjalsen I, Kauffman RF, Christiansen C. Raloxifene inhibits aortic accumulation of cholesterol in ovariectomized, cholesterol-fed rabbits. Circulation. 1997; 96:1964–1969. [PubMed: 9323087]
9. Bjarnason NH, Haarbo J, Byrjalsen I, Kauffman RF, Knadler MP, Christiansen C. Raloxifene reduces atherosclerosis: studies of optimized raloxifene doses in ovariectomized, cholesterol-fed rabbits. Clin Endocrinol (Oxf). 2000; 52:225–233. [PubMed: 10671951]
10. Manson JE, Allison MA, Rossouw JE, Carr JJ, Langer RD, Hsia J, Kuller LH, Cochrane BB, Hunt JR, Ludlam SE, Pettinger MB, Gass M, Margolis KL, Nathan L, Ockene JK, Prentice RL, Robbins J, Stefanick ML. Estrogen therapy and coronary-artery calcification. The New England journal of medicine. 2007; 356:2591–2602. [PubMed: 17582069]
11. Anderson GL, Limacher M, Assaf AR, Bassford T, Beresford SA, Black H, Bonds D, Brunner R, Brzyski R, Caan B, Chlebowski R, Curb D, Gass M, Hays J, Heiss G, Hendrix S, Howard BV, Hsia J, Hubbell A, Jackson R, Johnson KC, Judd H, Kotchen JM, Kuller L, LaCroix AZ, Lane D, Langer RD, Lasser N, Lewis CE, Manson J, Margolis K, Ockene J, O'Sullivan MJ, Phillips L, Prentice RL, Ritenbaugh C, Robbins J, Rossouw JE, Sarto G, Stefanick ML, Van Horn L, Wactawski-Wende J, Wallace R, Wassertheil-Smoller S. Effects of conjugated equine estrogen in postmenopausal women with hysterectomy: the Women's Health Initiative randomized controlled trial. Jama. 2004; 291:1701–1712. [PubMed: 15082697]
12. LaRosa JC, Grundy SM, Waters DD, Shear C, Barter P, Fruchart JC, Gotto AM, Greten H, Kastelein JJ, Shepherd J, Wenger NK. Intensive lipid lowering with atorvastatin in patients with stable coronary disease. The New England journal of medicine. 2005; 352:1425–1435. [PubMed: 15755765]
13. Raggi P, Davidson M, Callister TQ, Welty FK, Bachmann GA, Hecht H, Rumberger JA. Aggressive versus moderate lipid-lowering therapy in hypercholesterolemic postmenopausal women: Beyond Endorsed Lipid Lowering with EBT Scanning (BELLES). Circulation. 2005; 112:563–571. [PubMed: 16009795]
14. Zhou S, Turgeman G, Harris SE, Leitman DC, Komm BS, Bodine PV, Gazit D. Estrogens activate bone morphogenetic protein-2 gene transcription in mouse mesenchymal stem cells. Mol Endocrinol. 2003; 17:56–66. [PubMed: 12511606]
15. Garfinkel A, Tintut Y, Petrasek D, Bostrom K, Demer LL. Pattern formation by vascular mesenchymal cells. Proceedings of the National Academy of Sciences of the United States of America. 2004; 101:9247–9250. [PubMed: 15197273]
16. Emmanuele L, Ortmann J, Doerflinger T, Traupe T, Barton M. Lovastatin stimulates human vascular smooth muscle cell expression of bone morphogenetic protein-2, a potent inhibitor of low-density lipoprotein-stimulated cell growth. Biochemical and biophysical research communications. 2003; 302:67–72. [PubMed: 12593849]
17. Abedin M, Tintut Y, Demer LL. Vascular calcification: mechanisms and clinical ramifications. Arterioscler Thromb Vasc Biol. 2004; 24:1161–1170. [PubMed: 15155384]
18. Viles-Gonzalez JF, Fuster V, Corti R, Valdiviezo C, Hutter R, Corda S, Anand SX, Badimon JJ. Atherosclerosis regression and TP receptor inhibition: effect of S18886 on plaque size and composition--a magnetic resonance imaging study. Eur Heart J. 2005; 26:1557–1561. [PubMed: 15734766]
19. Corti R, Osende JI, Fallon JT, Fuster V, Mizsei G, Jneid H, Wright SD, Chaplin WF, Badimon JJ. The selective peroxisomal proliferator-activated receptor-gamma agonist has an additive effect on plaque regression in combination with simvastatin in experimental atherosclerosis: in vivo study by high-resolution magnetic resonance imaging. Journal of the American College of Cardiology. 2004; 43:464–473. [PubMed: 15013132]

20. Corti R, Osende J, Hutter R, Viles-Gonzalez JF, Zafar U, Valdivieso C, Mizsei G, Fallon JT, Fuster V, Badimon JJ. Fenofibrate induces plaque regression in hypercholesterolemic atherosclerotic rabbits: In vivo demonstration by high-resolution MRI. Atherosclerosis. 2006
21. Zhang Z, Machac J, Helft G, Worthley SG, Tang C, Zaman AG, Rodriguez OJ, Buchsbaum MS, Fuster V, Badimon JJ. Non-invasive imaging of atherosclerotic plaque macrophage in a rabbit model with F-18 FDG PET: a histopathological correlation. BMC Nucl Med. 2006; 6:3. [PubMed: 16725052]
22. Helft G, Worthley SG, Fuster V, Fayad ZA, Zaman AG, Corti R, Fallon JT, Badimon JJ. Progression and regression of atherosclerotic lesions: monitoring with serial noninvasive magnetic resonance imaging. Circulation. 2002; 105:993–998. [PubMed: 11864931]
23. Helft G, Worthley SG, Fuster V, Zaman AG, Schechter C, Osende JI, Rodriguez OJ, Fayad ZA, Fallon JT, Badimon JJ. Atherosclerotic aortic component quantification by noninvasive magnetic resonance imaging: an in vivo study in rabbits. Journal of the American College of Cardiology. 2001; 37:1149–1154. [PubMed: 11263622]
24. Choi BG, Vilahur G, Cardoso L, Fritton JC, Ibanez B, Zafar MU, Yadegar D, Speidl WS, Schaffler MB, Fuster V, Badimon JJ. Ovariectomy Increases Vascular Calcification Via the OPG/RANKL Cytokine Signaling Pathway. European Journal of Clinical Investigation. 2008 (in press).
25. Fritton, JC.; Chinitz, N.; Berman, D.; McNamara, LM.; Choi, BG.; Badimon, JJ.; Schaffler, MB. Atherogenic treatment impairs age-related cortical bone adaptation in female rabbits. Journal of Orthopaedic Research. 2007. http://www.ors.org/web/Transactions/53/1396.PDF: Abstract
26. Choi BG, Novoselsky CA, Vilahur G, Viles-Gonzalez JF, Zafar MU, Ibanez B, Fuster V, Badimon JJ. Validation study of a semi-automated program for quantification of atherosclerotic burden. Journal of Cardiovascular Magnetic Resonance. 2007 (in press).
27. Galvez A, Badimon L, Badimon JJ, Fuster V. Electrical aggregometry in whole blood from human, pig and rabbit. Thromb Haemost. 1986; 56:128–132. [PubMed: 3810551]
28. Toussaint JF, Southern JF, Fuster V, Kantor HL. T2-weighted contrast for NMR characterization of human atherosclerosis. Arterioscler Thromb Vasc Biol. 1995; 15:1533–1542. [PubMed: 7583524]
29. Pearlman JD, Zajicek J, Merickel MB, Carman CS, Ayers CR, Brookeman JR, Brown MF. High-resolution 1H NMR spectral signature from human atheroma. Magn Reson Med. 1988; 7:262–279. [PubMed: 3205143]
30. Wolf RL, Wehrli SL, Popescu AM, Woo JH, Song HK, Wright AC, Mohler ER 3rd, Harding JD, Zager EL, Fairman RM, Golden MA, Velazquez OC, Carpenter JP, Wehrli FW. Mineral volume and morphology in carotid plaque specimens using high-resolution MRI and CT. Arterioscler Thromb Vasc Biol. 2005; 25:1729–1735. [PubMed: 15947239]
31. Otsu N. A threshold selection method from gray-level histograms. IEEE Trans Systems, Man, and Cybernetics. 1979; 9:62–66.
32. Fujii K, Carlier SG, Mintz GS, Takebayashi H, Yasuda T, Costa RA, Moussa I, Dangas G, Mehran R, Lansky AJ, Kreps EM, Collins M, Stone GW, Moses JW, Leon MB. Intravascular ultrasound study of patterns of calcium in ruptured coronary plaques. Am J Cardiol. 2005; 96:352–357. [PubMed: 16054456]
33. Barkhem T, Carlsson B, Nilsson Y, Enmark E, Gustafsson J, Nilsson S. Differential response of estrogen receptor alpha and estrogen receptor beta to partial estrogen agonists/antagonists. Mol Pharmacol. 1998; 54:105–112. [PubMed: 9658195]
34. Seli E, Pehlivan T, Selam B, Garcia-Velasco JA, Arici A. Estradiol down-regulates MCP-1 expression in human coronary artery endothelial cells. Fertil Steril. 2002; 77:542–547. [PubMed: 11872210]
35. Belton O, Fitzgerald DJ. Cyclooxygenase isoforms and atherosclerosis. Expert reviews in molecular medicine. 2003; 5:1–18. [PubMed: 14987412]
36. Solomon SD, McMurray JJ, Pfeffer MA, Wittes J, Fowler R, Finn P, Anderson WF, Zauber A, Hawk E, Bertagnolli M. Cardiovascular risk associated with celecoxib in a clinical trial for colorectal adenoma prevention. The New England journal of medicine. 2005; 352:1071–1080. [PubMed: 15713944]

37. Jayachandran M, Mukherjee R, Steinkamp T, LaBreche P, Bracamonte MP, Okano H, Owen WG, Miller VM. Differential effects of 17beta-estradiol, conjugated equine estrogen, and raloxifene on mRNA expression, aggregation, and secretion in platelets. Am J Physiol Heart Circ Physiol. 2005; 288:H2355–2362. [PubMed: 15653758]

38. Polini N, Rauschemberger MB, Mendiberri J, Selles J, Massheimer V. Effect of genistein and raloxifene on vascular dependent platelet aggregation. Molecular and cellular endocrinology. 2007; 267:55–62. [PubMed: 17306449]

39. Blumenthal RS, Baranowski B, Dowsett SA. Cardiovascular effects of raloxifene: the arterial and venous systems. Am Heart J. 2004; 147:783–789. [PubMed: 15131531]

40. Riggs BL, Hartmann LC. Selective estrogen-receptor modulators -- mechanisms of action and application to clinical practice. The New England journal of medicine. 2003; 348:618–629. [PubMed: 12584371]

41. Corti R, Fuster V, Fayad ZA, Worthley SG, Helft G, Smith D, Weinberger J, Wentzel J, Mizsei G, Mercuri M, Badimon JJ. Lipid lowering by simvastatin induces regression of human atherosclerotic lesions: two years' follow-up by high-resolution noninvasive magnetic resonance imaging. Circulation. 2002; 106:2884–2887. [PubMed: 12460866]

42. Hodgin JB, Krege JH, Reddick RL, Korach KS, Smithies O, Maeda N. Estrogen receptor alpha is a major mediator of 17beta-estradiol's atheroprotective effects on lesion size in Apoe−/− mice. The Journal of clinical investigation. 2001; 107:333–340. [PubMed: 11160157]

43. Mayer LP, Devine PJ, Dyer CA, Hoyer PB. The follicle-deplete mouse ovary produces androgen. Biology of reproduction. 2004; 71:130–138. [PubMed: 14998904]

44. Bellino FL. Nonprimate animal models of menopause: workshop report. Menopause (New York, NY. 2000; 7:14–24.

45. Mayer LP, Dyer CA, Eastgard RL, Hoyer PB, Banka CL. Atherosclerotic lesion development in a novel ovary-intact mouse model of perimenopause. Arteriosclerosis, thrombosis, and vascular biology. 2005; 25:1910–1916.

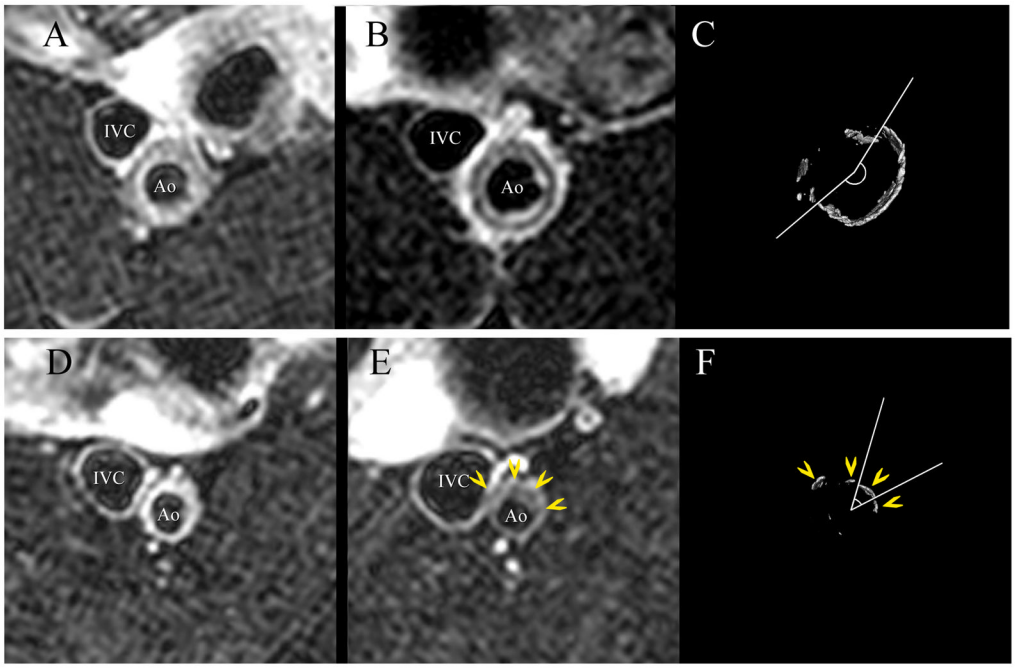

Figure 1.

Representative axial MRI and μCT images of the abdominal aorta. Raloxifene treatment (**upper panels**) resulted in a ring of calcification seen as low signal intensity within the vessel wall in the T2-weighted image (**B**) and confirmed in the matching μCT image (**C**). The distribution of calcification in the control OVX aortas was less organized and more nodular (**E, F**); yellow arrowheads identify matching calcifications. Corresponding pre-treatment MR images are seen in panels (**A**) and (**D**). The largest arc of calcification was measured for each μCT image (**C, F**). **Ao:** aorta; **IVC:** inferior vena cava.

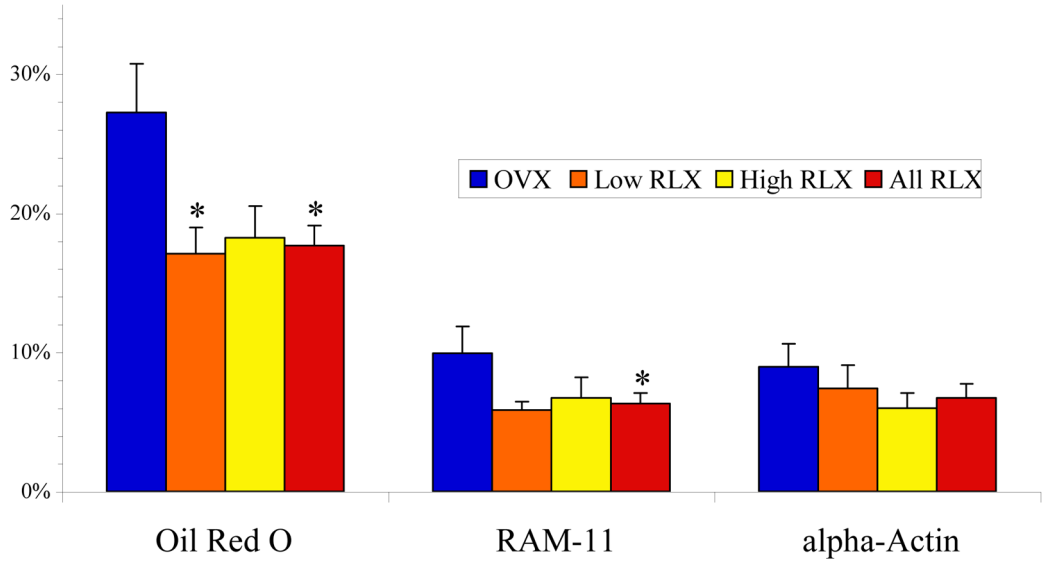

Figure 2.

Histopathologic analysis of aortic vessel wall composition. Oil Red O positive area corresponds to lipid deposition, RAM-11 to macrophage content, and α-actin to smooth muscle. *p<0.05 versus OVX. All values expressed as mean percent area ± SEM for each treatment group. **OVX:** ovariectomized control group (n=12); **RLX:** raloxifene therapy group (**Low**: low-dose, n=12, **High**: high-dose, n=12).

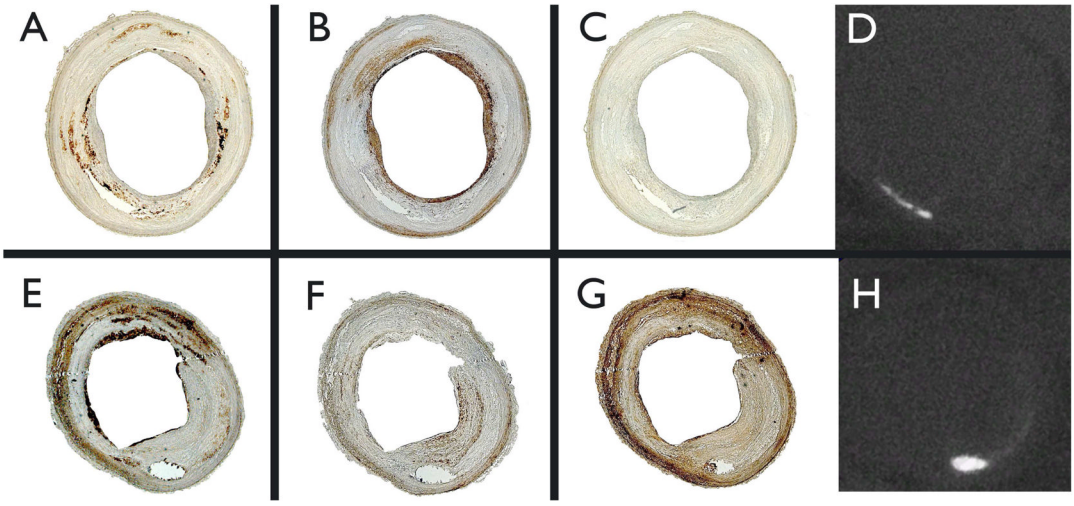

Figure 3.

Representative immunohistopathology photomicrographs of axial sections of the abdominal aorta with corresponding μCT images demonstrating location of calcification. Upper panels are from a raloxifene-treated animal; lower panels, from ovariectomized control. RAM-11 staining for macrophages are seen in panels **(A)** and **(E)**; α-actin for smooth muscle cells, panels **(B)** and **(F)**; matrix metalloproteinase-1 (MMP-1), panels **(C)** and **(G)**; μCT, panels **(D)** and (**H)**.

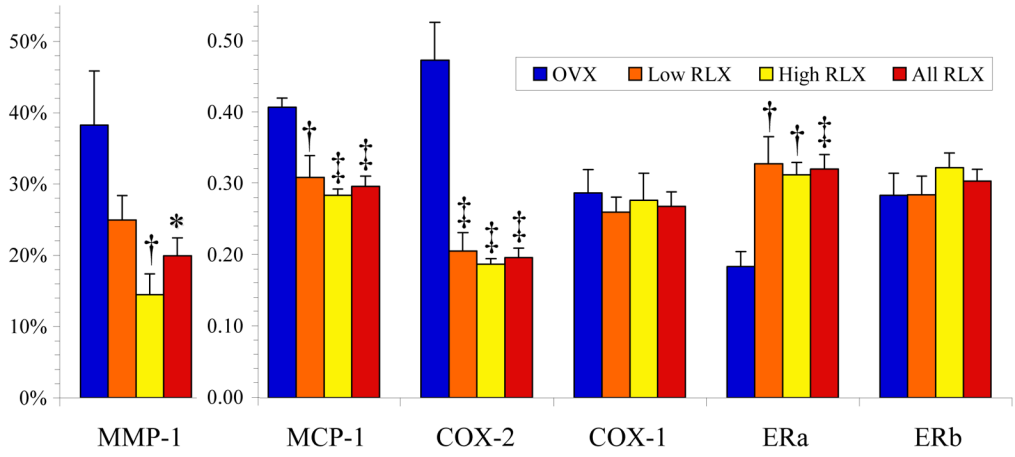

Figure 4.

Plaque activity assessed by immunohistochemistry for matrix metalloproteinase-1 (MMP-1) [%vessel wall staining positively ± SEM] and by Western blot analysis for monocyte chemoattractant protein-1 (MCP-1), cyclooxygenase-2 (COX-2), cyclooxygenase-1 (COX-1), estrogen receptor-α (ERa) and estrogen receptor-β (ERb) protein expression [Arbitrary Units ± SEM]; *p<0.05, †p<0.01, and ‡p<0.001 versus OVX. **OVX:** ovariectomized control group (n=12); **RLX:** raloxifene therapy group (**Low**: low-dose, n=12, **High**: high-dose, n=12).

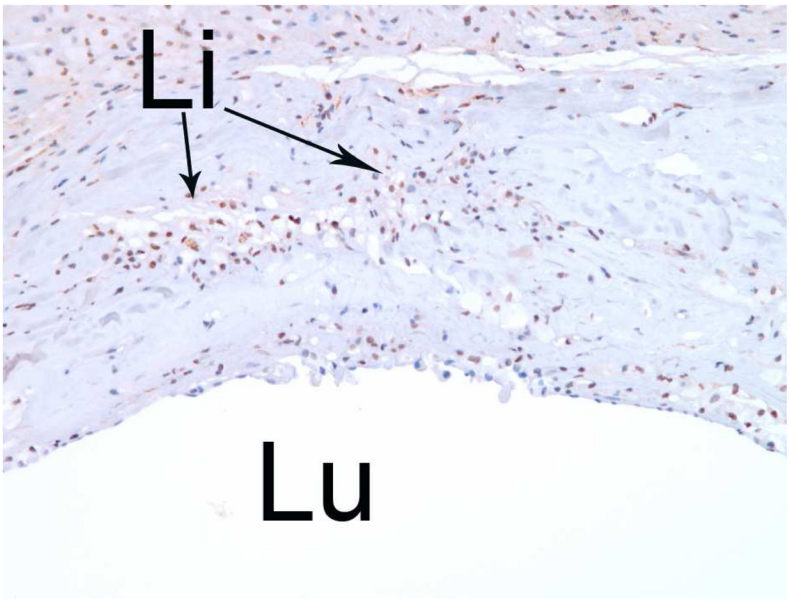

Figure 5.
Increased nuclear staining of estrogen receptor-α (ERa), with brown-stained nuclei, is highly specific to the inflammatory infiltrative cells within the atherosclerotic aorta as seen in cross section by light microscopy (10x). **Lu**: lumen; **Li**: lipid pools.

Table 1

End-of-follow-up serum plasma lipid levels.

	OVX (n=12)	RLX (n=24)	p
Total Cholesterol	573 ± 88	520 ± 59	0.61
LDL-Cholesterol	454 ± 62	403 ± 48	0.53
HDL-Cholesterol	55 ± 9	73 ± 9	0.25
Triglycerides	67 ± 24	58 ± 10	0.70
LDL:HDL Ratio	9.3 ± 0.5	6.6 ± 0.5	0.004

All serum lipid values expressed as mg/dl ± SEM, $p<0.05$ considered statistically significant. **OVX:** ovariectomized control group; **RLX:** raloxifene therapy group.

Table 2

Changes in vessel wall dimensions from baseline to end-of-follow-up as assessed by MRI.

	Lumen Area	Vessel Wall Area
OVX (n=12)	−1.2 ± 7.5%	−1.9 ± 3.4%
Low RLX (n=12)	−0.5 ± 13.5%	−4.8 ± 6.4%
High RLX (n=12)	−1.4 ± 17.4%	−6.2 ± 6.6%
All RLX (n=24)	−0.9 ± 10.7%	−5.5 ± 4.5% *

All values expressed as the percent change ± SEM between baseline (at randomization) and end-of-follow-up.

* $p<0.05$ versus baseline.

OVX: ovariectomized control group; **RLX:** raloxifene therapy group (**Low**: low-dose, **High**: high-dose).

Table 3

Quantitative analysis of vessel calcification by μCT and corresponding bone morphogenetic protein-2 (BMP-2) expression by Western blot analysis.

	Mineral Density (mg/cm^3)	Particle Density (particles/cm^3)	Calcific Arc Angle	BMP-2 (Arbitrary Units)
OVX (n=12)	8.4 ± 2.8	94 ± 26	33 ± 7°	37.7 ± 0.1
Low RLX (n=12)	6.4 ± 2.1	89 ± 27	67 ± 10° *	62.5 ± 0.1
High RLX (n=12)	5.8 ± 2.0	79 ± 23	60 ± 11°	53.9 ± 0.1
All RLX (n=12)	6.1 ± 1.4	85 ± 17	63 ± 7° †	58.2 ± 0.1 *

All values expressed as mean ± SEM;

* p<0.05 and

† p<0.01 versus OVX.

OVX: ovariectomized control group; **RLX:** raloxifene therapy group (**Low**: low-dose, **High**: high-dose).